

THE PHYSICAL REVIEW

A journal of experimental and theoretical physics established by E. L. Nichols in 1893

SECOND SERIES, VOL. 148, No. 3

19 AUGUST 1966

Branching Ratios in C^{14} and $N^{14}\dagger$

R. R. CARLSON

Department of Physics and Astronomy, University of Iowa, Iowa City, Iowa

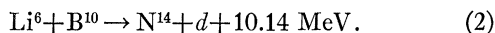
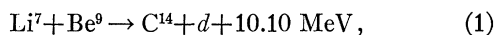
(Received 4 April 1966)

The $Be^9(Li^7,d)C^{14}$ and $B^{10}(Li^6,d)N^{14}$ reactions were used as sources of gamma-emitting excited states of C^{14} and N^{14} . Three-parameter measurements of E , dE/dx , and E_γ in $1024 \times 1024 \times 256$ -channel detail were used to identify deuteron groups and the gamma rays associated with them. Radiation from six bound levels in C^{14} and from eight bound levels in N^{14} was analyzed to give branching ratios. Results are generally in agreement with previous measurements where they have been made. Two unbound levels in N^{14} are found to gamma-decay in competition with proton decay.

I. INTRODUCTION

THE characteristics of C^{14} and N^{14} states have been studied by the use of a number of different nuclear reactions.¹ In particular, the gamma decay of the excited states has been studied in considerable detail. This interest has been stimulated by rather detailed calculations of the wave functions of these states.²⁻⁴ These calculations are based on the assumption of a C^{12} core with two nucleons outside. Surprisingly pure jj -coupled two-particle wave functions have been found to describe the states below 10-MeV excitation. Information on gamma-decay transition probabilities serves as a sensitive test of such wave functions. In the present work, the excited states of C^{14} and N^{14} have been studied by the use of lithium-induced nuclear reactions, which makes possible the population of these states in a new way.

The reactions used were



Each of these reactions has many other outgoing channels. The gamma-ray spectra resulting from all of these

channels have been studied in this laboratory⁵; because of the complexity of the spectra, it was not possible to completely disentangle the various gamma-ray lines, even with the use of a three-crystal pair spectrometer. In the present work, the gamma-ray spectra were obtained in coincidence with the particle groups and the particles were identified by measurement of both E and dE/dx . By this means the complex gamma-ray spectra are drastically simplified and branching ratios for decay of individual nuclear states can be obtained.

One advantage of lithium-induced nuclear reactions for this sort of investigation is that levels in the residual nuclei are generally populated unless forbidden by isotopic-spin selection rules. Recent work on the lithium-boron reactions in this laboratory has shown that the lower levels of the residual nuclei tend to be formed with a cross section proportional to $2J+1$, where J is the residual nuclear spin.⁶ More recent unpublished work in this laboratory shows this is also true of the lithium-beryllium reactions. Under these circumstances one would expect observable amounts of gamma radiation from any bound residual nucleus level if such a level exists and if gamma radiation is possible. The failure to observe a group, when other similar groups are being formed in amounts determined essentially by phase-space considerations, is a strong argument for the non-existence of such a group.

[†] Supported in part by the National Science Foundation.

¹ T. Lauritsen and F. Ajzenberg-Selove, in *Nuclear Data Sheets*, compiled by K. Way *et al.* National Academy of Sciences—National Research Council, Washington, D. C., 1962), NRC 61-5-6.

² W. W. True, *Phys. Rev.* **130** 1530 (1963).

³ E. K. Warburton and W. T. Pinkston, *Phys. Rev.* **118**, 735 (1960).

⁴ I. Unna and I. Talmi, *Phys. Rev.* **112**, 452 (1958).

⁵ E. Norbeck, S. A. Coon, R. R. Carlson, and E. Berkowitz, *Phys. Rev.* **130**, 1971 (1963).

⁶ R. R. Carlson and R. L. McGrath, *Phys. Rev. Letters* **15**, 173 (1965).

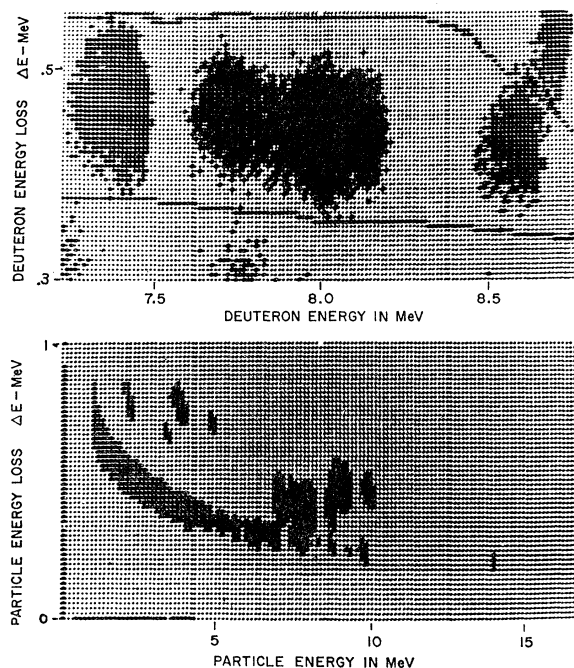


FIG. 1. (Top) Contour display of dE/dx versus E for charge-one reaction products (mostly deuterons) in coincidence with gamma radiation or neutrons for the $\text{Li}^7 + \text{Be}^9$ reaction. Heavily darkened points correspond to the 16 or more count level. The darkened lines running across the display mark the upper and lower boundaries of the region recognized by the computer as corresponding to deuterons. The deuteron groups appearing in this picture correspond, from left to right, to the 7.34-, 7.01-, 6.98-, 6.72-, 6.59-, and 6.09-MeV excited states of C^{14} . Not all are resolved. The group in the extreme upper right corner is due to $\text{Be}^9(\text{Li}^7, p)\text{C}^{13}$ (3.68-3.85) reaction. (Bottom) Condensed display of all dE/dx -versus- E data for coincident charge-one reaction products for the $\text{Li}^7 + \text{Be}^9$ reaction. The count level is 128 or more here. Top picture corresponds to middle region of this picture.

Isotopic-spin selection rules would be expected to forbid the formation of $T=1$ states in N^{14} in the second reaction. In a report⁷ on an early stage of this work it was stated that this rule apparently broke down for the 9.16-MeV state of N^{14} since gamma-ray decay of this state apparently was observed. Since that time several new states have been observed in this excitation region.⁸ One is at 9.13 MeV and another is at 8.96 MeV and both are $T=0$ states. These states are both formed in the second reaction⁹ and the latter gamma decays. In addition, the $\text{B}^{11}(\text{Li}^6, d)\text{N}^{15}$ (9.17) reaction has a very high yield⁹ and the target used in the early work had about 10% B^{11} contaminant. The deuteron group from this reaction could have been confused with that corresponding to the $\text{B}^{10}(\text{Li}^6, d)\text{N}^{14}$ (9.16) reaction because of poor resolution. Lack of resolution in the earlier work

⁷ R. R. Carlson, in *Comptes Rendus du Congrès International de Physique Nucléaire, Paris, 1964*, edited by P. Gungunberger (Centre National de la Recherche Scientifique, Paris, 1964), Vol. II, p. 1087.

⁸ R. W. Detenbeck, J. C. Armstrong, A. S. Figuerra, and J. B. Marion, *Nucl. Phys.* **72**, 552 (1965).

⁹ R. L. McGrath, *Phys. Rev.* **145**, 802 (1966).

led to the incorrect conclusion. Good-resolution work⁹ on the particle spectra in the $\text{B}^{10}(\text{Li}^6, d)\text{N}^{14}$ reaction shows that none of the known $T=1$ states of N^{14} are formed with more than a few percent of the intensity of the $T=0$ states.

Because of the characteristics of the lithium-induced reactions, the work described below gives the gamma-decay spectra of the $A=14$ energy levels in two parts. The $T=1$ levels, of course, come from the first reaction which produces C^{14} . The $T=0$ levels come from the second reaction. In the latter case this feature serves to simplify the spectra since the number of levels contributing to the gamma spectrum is reduced.

II. METHOD AND RESULTS

The University of Iowa 5.5-MV Van de Graaff was used to accelerate the lithium particles used in the nuclear reactions studied in this work. The beam energy was 5.0 MeV in the case of the Li^7 bombardment and 5.6 MeV in the case of the Li^6 bombardment. The beam energy has proven to be constant to within 5 keV over

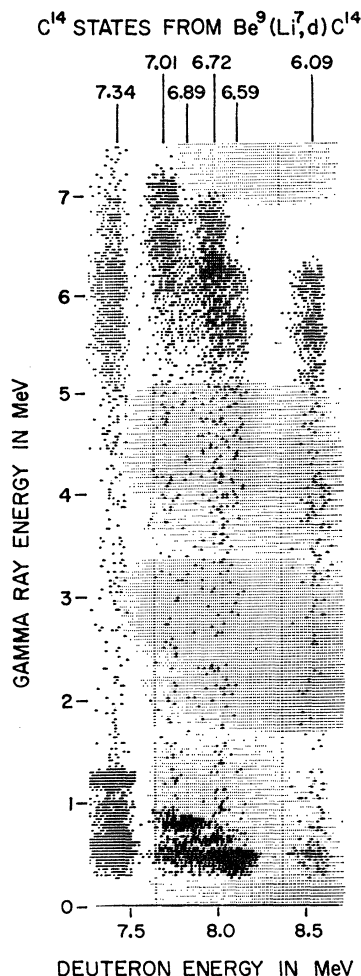


FIG. 2. Contour display of E_γ versus E_d in full detail with 256×128 channels. The 128 channels for E_d are $\frac{1}{3}$ of the total 1024 channels in the original data. This display is pieced together out of 5 scans of the data tape. Contour level is 4 counts here.

long bombarding periods in previous work.⁹ Targets were about 100 keV thick for 5-MeV Li ions.

The target chamber has been described in detail before.¹⁰ Briefly, it is a cylindrical pillbox 5 cm in radius with the target on the axis and the beam incident on the target at right angles to the axis. A solid-state, E - dE/dx detector system is mounted inside the target chamber and can be located at any angle with respect to the beam from 0 to 140 deg. It is 2.5 cm from the target. In the present work, it is at 15 deg to the beam direction. The E detector defines the solid angle, being 5 mm in diameter at a distance of 2 cm. The dE/dx counter is 0.0025 cm thick. Aluminum absorbing foils of various thicknesses can be placed in front of the particle-detector system.

A 12.5-cm-diam \times 15-cm-long NaI(Tl) crystal is used for gamma-ray detection. This crystal can be placed at any angle with respect to the beam from 0 to 110 deg on either side of the beam direction, when it is up tight against the target-chamber wall (5.2 cm from the target). Data were taken with it in several positions. The gamma detector was placed at 35 deg on the opposite side of the beam to the particle-detector system, and at 45 and 110 deg on the same side. These directions approximately correspond to the emission of gamma rays at 0°, 90°, and 145°, respectively, with respect to the direction of the residual nuclei. The gamma-ray crystal subtends a large solid angle at the target; the 12.5-cm-diam circular area in the middle of the crystal,

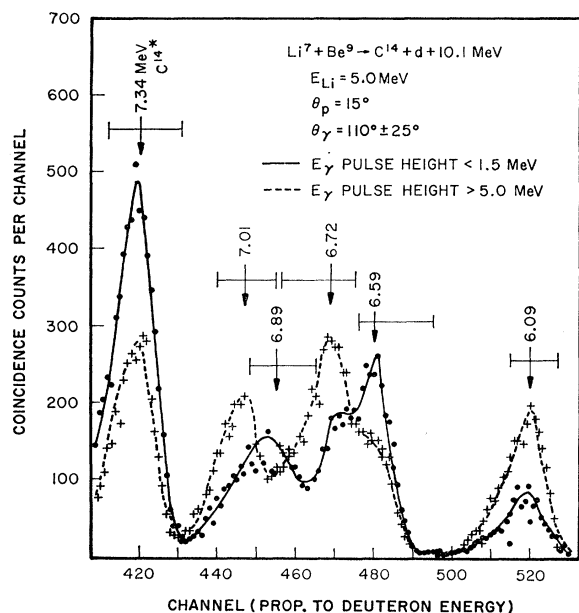


FIG. 3. Sums of contour data shown in Fig. 2 for different gamma-ray energies. Numbers on arrows indicate state in C^{14} to which deuteron group corresponds. Horizontal bar indicates range of deuteron energy summed over in later figures.

¹⁰ V. P. Hart, E. Norbeck, and R. R. Carlson, Phys. Rev. **137**, B17 (1965).

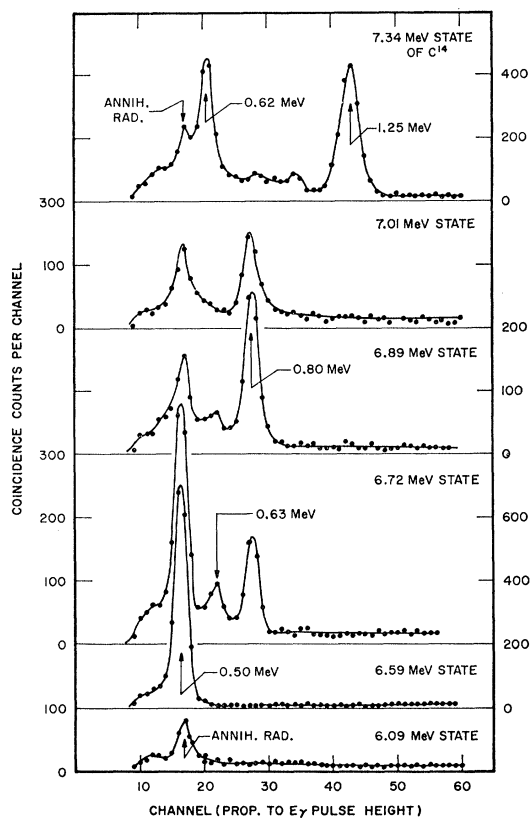


FIG. 4. Low-energy gamma-ray pulse-height distributions for various excited states of C^{14} . These distributions were obtained by summing the information contained in the contour shown in Fig. 2 over the particle pulse heights shown in Fig. 3. Because of inadequate particle resolution gamma-ray peaks belonging to one state appear in the distributions of neighboring states. Peaks are labeled when they correspond to the photopeak of a gamma ray associated with the state under consideration.

at a distance of 12.7 cm from the target, subtends an angle of 52 deg. With this large an angular coverage, it is expected that all but the strongest angular correlations would be wiped out with the angles of observation used. This is even truer of the low-energy gamma rays which would be primarily captured in the front part of the crystal; the angle subtended by the front part of the crystal in the reaction plane is 100°. No differences in branching ratios were observed at the various angles of observation which were more than 10%. Averages were taken where differences were observed.

In order to pick the gamma transitions of interest out of the large number of gamma rays present, measurements are made of three parameters associated with each event detected. Particles are detected in coincidence with gamma rays (50 nsec resolving time) using conventional electronics which have previously been described.¹⁰ Pulse heights from the three detectors for particle energy, energy-loss rate, and gamma-ray energy are analyzed in three separate pulse-height analyzers with 1024-, 1024-, and 256-channel detail, respectively. An on-line computer (CDC 160A) sorts these pulse

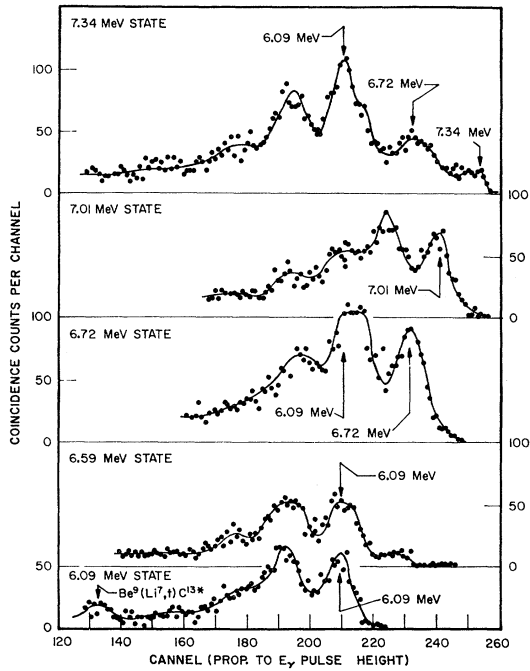


Fig. 5. High-energy gamma-ray pulse-height distribution for various excited states of C^{14} . See caption in Fig. 4.

heights giving an immediate two-parameter display of the data for monitoring purposes. The three parameters are stored on magnetic tape in full detail for later analysis. This analysis is performed with the same computer. Details of the method of analysis have been described before.¹⁰

One of the results of the above analysis is a two-parameter presentation of the data which shows dE/dx versus E for all the particles detected. The lower part of Fig. 1 shows a polaroid picture of this aspect of the data for the $Li^7 + Be^9$ reaction. The charge-1 particles are shown only. Various states of the residual carbon

nuclei show up here as populated spots on the ionization curves for protons, deuterons, and tritons. Only particles coincident with gamma rays appear here so the ground-state groups are not seen. Full scale on horizontal E axis is 16 MeV; on the dE/dx axis it is 1.0 MeV. The upper part of Fig. 1 shows an enlargement of a 15×16 -channel section in the lower part corresponding to the deuterons associated with bound C^{14} states. The enlargement shows a 59×128 -channel section out of the 1024×1024 detail in which the data is actually recorded.

The computer is also used to form two-parameter displays of E_γ versus E for particular particle types. Using the ionization curve information shown in Fig. 1, the computer was programmed to select particle types and display the gamma-ray pulse heights associated with particles of known type and energy. Figure 2 shows such a display. The particles in this case are the deuterons associated with the bound states of C^{14} . The particle energy E , is plotted horizontally in 128 channels and covers the same range as in the upper part of Fig. 1. Gamma-ray energy covers the range from 0 to 7.5 MeV in 256 channels. This is a contour picture and shows the presence of both ground state and cascade gamma decay.

Particle resolution is not adequate to separate all of the states so that gamma-decay branching ratios can be determined accurately. This is a result of compromise between target thickness and adequate statistics. However, it is possible to see that certain cascade decays belong to one level rather than the other because of the two parameter nature of the E_γ -versus- E data and the fact that some levels decay primarily by low-energy radiation while others decay by high-energy radiation.

The data were also summed by the computer over the ranges indicated in Fig. 3 to give pulse-height distributions. It is from these, together with due allowance for particle resolution, that the following results are obtained. Figure 4 shows the low-energy pulse-height distributions for the various C^{14} states and Figure 5 shows

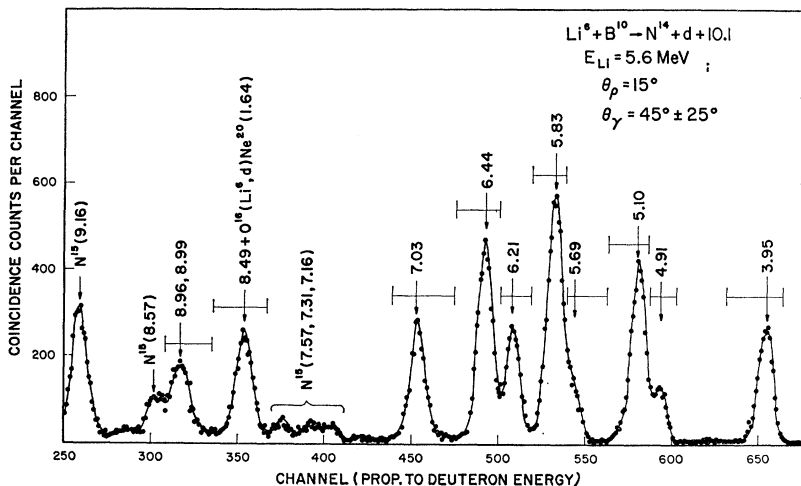


FIG. 6. Number of deuteron-gamma coincidences versus deuteron energy for $B^{10}(Li^6, d)N^{14}$ reaction. Numbers on arrows indicate excitation of N^{14} state associated with deuteron group. Horizontal bar indicates range of deuteron energy summed over in later figures.

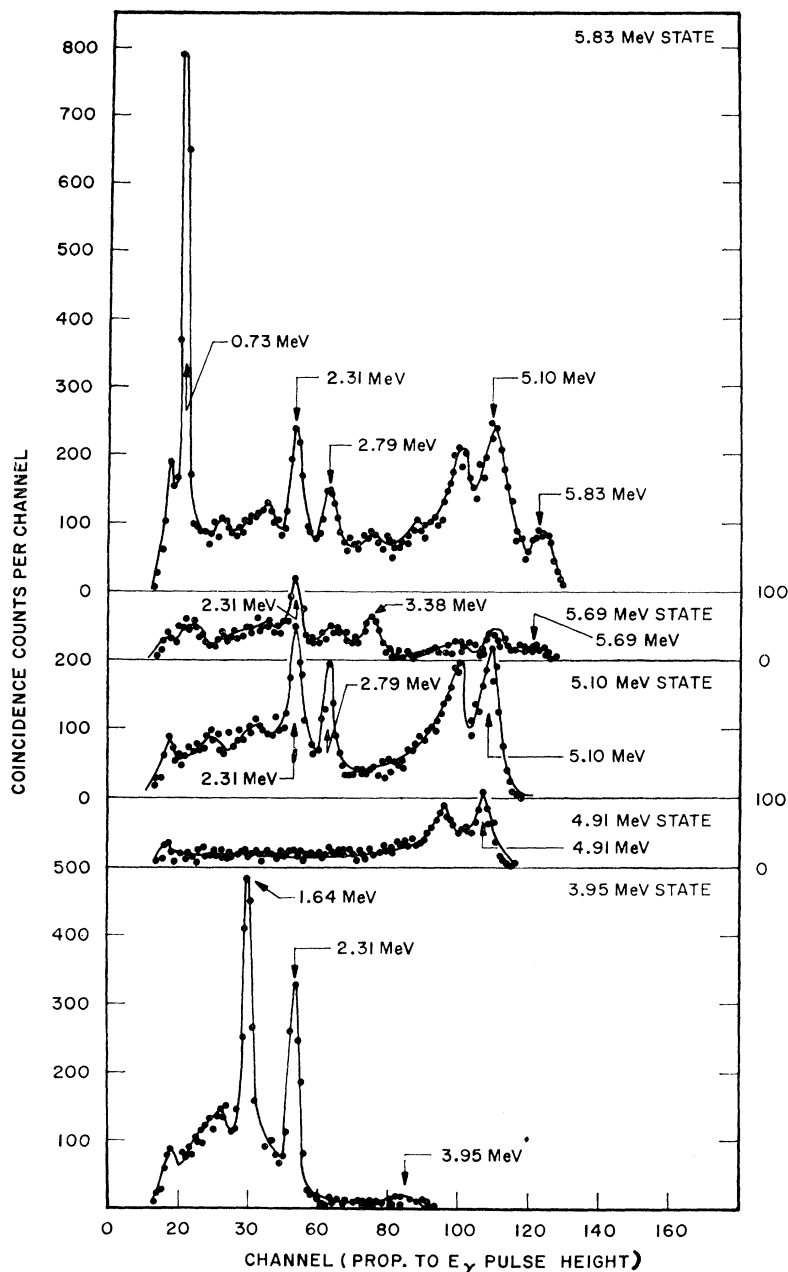


FIG. 7. Gamma-ray pulse-height distributions for various excited states of N^{14} . Peaks are labeled when they correspond to the photopeak of a gamma ray associated with the state under consideration.

them for the high-energy case. No gamma rays are expected with energies between 1.25 and 6.09-MeV and none were observed except a small peak at 3.8 MeV which was due to the $Be^9(Li^7,t)C^{13}$ (3.8 MeV) reaction. In some cases the lack of resolution results in pulses from gamma decay of a neighboring state apparently giving rise to peaks in the pulse-height distribution of the state under consideration. Such peaks have not been labeled. In all cases a labeled peak at the same energy will be found in the pulse-height distribution corresponding to a neighboring state. Labeled peaks in a

pulse-height distribution are believed to be associated with the gamma-decay of the corresponding state.

The method used to study the states of N^{14} with the $B^{10}(Li^6,d)N^{14}$ reaction was identical to that used for the states of C^{14} . The results are shown in Fig. 6 in a manner similar to that used in Fig. 3 except that the particle groups in coincidence with gamma rays are shown here for all gamma-ray energies together instead of being shown for high- and low-energy gamma rays separately. Numbers on arrows indicate the excited states of N^{14} with which the deuteron groups are associated. Peaks

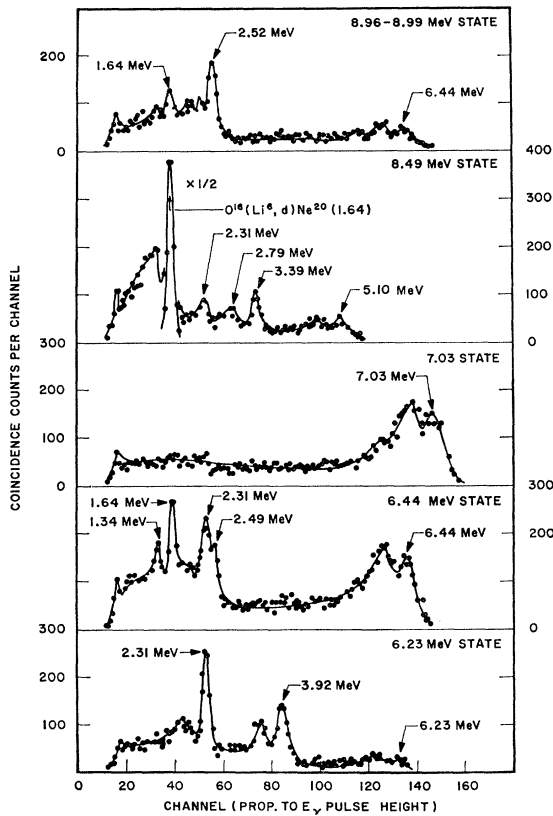


FIG. 8. See caption of Fig. 7.

labeled "N¹⁵" are due to the reaction B¹¹(Li⁶,d)N¹⁵ arising from B¹¹ in the target. The target was enriched B¹⁰ but there was about 10% B¹¹ contained in it. There is a small contribution to the peak labeled "8.96, 8.99" arising from the B¹¹(Li⁶,d)N¹⁵(8.32) reaction. The population of this N¹⁵ state is known⁹ and a correction for the contribution can be made. There is a contribution to the peak labeled "8.49" arising O¹⁶(Li⁶,d)Ne²⁰(1.64) reaction. The decay scheme of the 8.49-MeV level⁸ allows for a certain amount of 1.64-MeV radiation but most of that observed comes from the oxygen contaminant. However, the "8.49" peak is primarily due to coincidences with higher energy gamma rays associated with the cascade decay of the 8.49-MeV level of N¹⁴.

The pulse-height distributions, corresponding to the sums indicated by horizontal bars in Fig. 6, are shown on Figs. 7 and 8. All excited states of N¹⁴ up to and including the 7.03-MeV state have Q values large enough so that contaminating reactions cannot interfere. The accidental coincidence rate was also negligible. The pulse-height distributions shown in Figs. 7 and 8, and those in Figs. 4 and 5 also, as well as similar ones taken at other angles of observation can be used to determine the branching ratios of the various excited states provided one knows the relative efficiency of the NaI(Tl) detector for the gamma rays involved.

Relative photopeak efficiencies for NaI(Tl) have been calculated and measured under a variety of circumstances.¹¹ None of these matches the conditions of the present experiment exactly but one can interpolate to get approximate results. In addition, the gamma decay of the N¹⁴ states offers two cases where two gamma rays are one-to-one cascade: 3.95 state has 1.64- and 2.31-MeV gamma rays in cascade, 5.10-MeV state has 2.31 and 2.79 MeV. These can be used to obtain relative photopeak efficiencies for gamma-ray energies 1.64, 2.31, and 2.79 MeV. Further, the differential cross section for populating the various excited states has been measured at 4.9-MeV bombarding energy⁹ and preliminary work shows little variation in relative populations with bombarding energy. From the 4.91- and 7.03-MeV states, which decay overwhelmingly by ground-state decay, one can obtain relative photopeak efficiencies for the corresponding gamma rays by correcting the photopeak heights in Figs. 7 and 8 by the relative populations of the states and repeating for the other angles of observation. These several sources of information were used to construct a relative photopeak-efficiency curve from 1.64 to 7.03 MeV making use of the fact such a curve has to be a smooth curve. Knowing

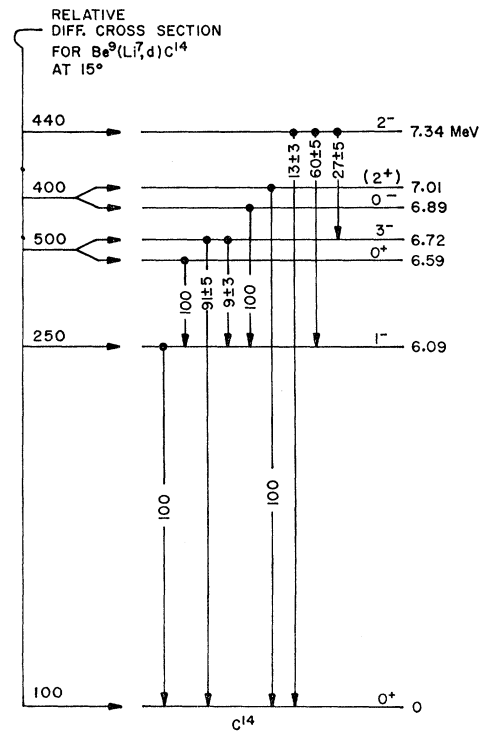


FIG. 9. Energy-level diagram for C¹⁴. Energy levels and spin-parity assignments obtained from Ref. 12. Differential cross-sections are from unpublished work at this laboratory. Branching ratios are from present work.

¹¹ R. L. Heath, AEC Research and Development Report IDO 16880-1 (unpublished); W. F. Miller, J. Reynolds, W. J. Snow, Argonne National Laboratory Report No. ANL-5902 (unpublished).

of Warburton *et al.*¹⁹ In the case of the 6.44-MeV level a branch to the 3.95-MeV level was suspected²⁰ and confirmed²¹ as well as a branch to the 5.10-MeV level. The present results are in agreement on the nature of the branching but the low-energy branch is slightly weaker and the ground-state branch slightly stronger in the present results. Recent work¹⁹ on the 7.03-MeV level has indicated a weak ($9 \pm 5\%$) branch to the 3.95-MeV state which is not seen here. However, a branch of as much as 5% is not ruled out by the present results.

The major portion of the gamma-ray decay of the two levels at 8.49- and 8.96 MeV is observed to be the same here as in previous work.⁸ However, a weak branch (about $\frac{1}{6}$) of the 8.49-MeV level to the 5.83-MeV level was not observed here. The gamma radiation from the unresolved pair of levels at 8.96 and 8.99 MeV is attributed to the 8.96-MeV member because of its known⁸ gamma-decay branching.

¹⁹ E. K. Warburton, J. S. Lopes, R. W. Ollerhead, A. R. Poletti, and M. F. Thomas, *Phys. Rev.* **138**, B104 (1965).

²⁰ H. J. Rose, *Nucl. Phys.* **19**, 113 (1960).

²¹ E. K. Warburton, J. W. Olness, D. W. Alburger, D. J. Bredin, and L. F. Chase, *Phys. Rev.* **134**, B338 (1964).

The observation in the present experiment of gamma decay from these levels, which are unbound to proton decay, argues that the proton width must be less than or comparable to the gamma width. A comparison of the coincident yield in Fig. 6 with the noncoincident yield⁹ shows that there is a noticeable reduction, in the coincident yield, of the relative height of the peaks corresponding to the unbound levels. The proton and gamma widths are, therefore, comparable. They are of the order of 0.01 eV in each case since these are the previously found⁸ gamma widths, approximately. Although these values will need modification, since it was assumed⁸ that the gamma widths were much less than the proton widths, they will still be of this order of magnitude.

Particle decay of the 8.49- and 8.96-MeV levels requires $l=4$ and $l=5$ proton waves, respectively. The penetrability of such high angular-momentum proton waves is sufficiently low that the proton widths of these levels could be of the above order of magnitude. The total widths of these states are not known, but their upper limits of <0.21 keV and <1 keV for the 8.49- and 8.96-MeV levels, respectively, are certainly consistent with the above very small proton widths.

Neutrons from Deuteron Breakup on He³

R. G. KERR

*University of Wisconsin, Madison, Wisconsin**

(Received 24 March 1966)

Neutron spectra produced by bombarding He³ with deuterons have been measured for bombarding energies from 7 to 12 MeV and neutron emission angles from 0 to 70 deg. The observed spectra exhibit no structure attributable to a state in Li⁴. An upper limit for the cross section for forming such a state is deduced.

INTRODUCTION

NEUTRON spectra produced when He³ is bombarded with deuterons were investigated. The existence of neutrons from deuteron breakup on He³ was first reported by Henkel *et al.*¹ for energies slightly above threshold. Rybakov *et al.*² have published a neutron spectrum taken at 18.6-MeV bombarding energy.

The present experiment was undertaken to study the energy distribution of the breakup neutrons as a function of bombarding energy and emission angle, and

to search for a possible analog state in Li⁴ to the excited states in the α particle.^{3,4}

Most experimental searches for Li⁴ have been either inconclusive or unsuccessful. A particle-stable Li⁴ almost certainly does not exist.⁵⁻⁸ Unbound states in

³ H. W. Lefevre, R. R. Borchers, and C. H. Poppe, *Phys. Rev.* **128**, 1328 (1962); C. H. Poppe, C. H. Holbrow, and R. R. Borchers, *ibid.* **129**, 733 (1963).

⁴ Additional references may be found in the following articles: He⁴ states—W. E. Meyerhof, *Rev. Mod. Phys.* **37**, 512 (1965) and Ref. 13; Li⁴ states—T. A. Tombrello, *Phys. Rev.* **138**, B40 (1965).

⁵ R. K. Sheline, *Phys. Rev.* **87**, 557 (1952).

⁶ H. Tyrén and P. A. Tove, *Phys. Rev.* **96**, 773 (1954).

⁷ S. Bashkin, R. W. Kavanagh, and P. D. Parker, *Phys. Rev. Letters* **3**, 518 (1959).

⁸ W. L. Imhof, F. J. Vaughn, L. F. Chase, Jr., H. A. Grench, and M. Walt, *Nucl. Phys.* **59**, 81 (1964).

* Work supported in part by the U. S. Atomic Energy Commission.

¹ R. L. Henkel, J. E. Perry, Jr., and R. K. Smith, *Phys. Rev.* **99**, 1050 (1955).

² B. V. Rybakov, V. A. Sidorov, and N. A. Vlasov, *Nucl. Phys.* **23**, 491 (1961).